Catalysis Today 142 (2009) 298–302

Contents lists available at ScienceDirect

Catalysis Today

journal homepage: www.elsevier.com/locate/cattod

# The effect of zirconium and niobium oxidic species on platinum dispersion in 1%Pt/Nb,Zr-containing MCM-41

Joanna Goscianska *, Ryszard Fiedorow, Agata Wawrzynczak, Maria Ziolek

*A. Mickiewicz University, Faculty of Chemistry, Grunwaldzka 6, 60-780 Poznan, Poland*

ARTICLE INFO

*Article history:*
Available online 27 September 2008

*Keywords:*
Mesoporous metallosilicates
Pt–$NbO_x$ interaction
Zr effect on morphology

ABSTRACT

Platinum was deposited on MCM-41 mesoporous supports that contained niobium and/or zirconium introduced either at the stage of mesoporous material synthesis or after synthesis by impregnation. It has been found that zirconium introduced during synthesis of MCM-41, influenced particle size of the material to a considerable extent and this, in turn, resulted in quite a high dispersion of platinum on the support. Such an effect was not observed in the case of niobiosilicate material. Niobium affected dispersion, when it was introduced to silicate MCM-41 by impregnation. Niobium oxidic species formed on mesoporous material surface, due to their strong interaction with platinum, prevented from sintering of the latter during reduction, thus increasing platinum dispersion.



## 1. Introduction

Catalytic properties of supported platinum are influenced by support materials because the support can have an important effect on the kind and dispersion of Pt species present on its surface [1–3]. Moreover, treatment conditions of the supported catalyst can change the Pt–support interaction and the nature of Pt species thus affecting the activity of platinum catalysts [1,2]. Recently, mesoporous MCM-41 materials have been used as supports for Pt particles (e.g. [2,3]). Unfortunately, the metal particles supported on the walls of mesoporous tubes are not stable and their migration results in sintering at high temperatures. The question arises whether other metal-containing species incorporated into mesoporous MCM-41 material affect platinum dispersion. The determination of the effect of the support and various treatment conditions on surface, internal structure and morphology is of a great importance to elucidating the mechanism of the metal–support interaction and the correlation between the structure of solids and surface properties.

In the recent paper [4], we have studied catalytic properties of platinum supported on Zr and/or Nb-containing MCM-41 materials and the significant role played by the chemical composition of the support in the catalytic activity of Pt species has been stressed. In this work we have focused on the dependence of platinum dispersion on calcination and reduction processes as well as on the nature of a metal (such as Zr and Nb) introduced into the support and the preparation method employed. The role of the morphology is also discussed. Zirconium and niobium were chosen as elements introduced into silicate MCM-41 by using co-precipitation and impregnation method. Niobia is well known as a strong metal–support interacting oxide [5] and therefore the location of Nb in the framework or extra-framework positions could significantly influence the interaction with platinum species.

## 2. Experimental

### 2.1. The preparation of samples—synthesis and modification

MCM-41 was synthesized by the hydrothermal method from sodium silicate (27% $SiO_2$ in 14% NaOH; Aldrich) and cetyltrimethylammonium chloride (25 wt.% aqueous solution; Aldrich) as a template. Trisoxalate ammonium complex of niobium (CBMM, Brazil) and $ZrO(NO_3)_2$ (Alfa Aesar) were used for the preparation of mono- and bimetallic silicates. The Si/T atomic ratio (T = Nb and/or Zr) in the gels was 128, when niobium and zirconium oxide species were introduced into MCM-41 either at the stage of the mesoporous material synthesis or by impregnation of MCM-41 with aqueous solutions of Nb and Zr compounds.

Incipient wetness technique was applied to impregnate all the materials with aqueous solution of hexachloroplatinic acid ($H_2PtCl_6{\cdot}H_2O$, Aldrich) in the amount necessary to obtain 1 wt.%

* Corresponding author. Tel.: +48 61 829 13 05; fax: +48 61 829 15 05.
*E-mail address:* asiagosc@amu.edu.pl (J. Goscianska).

0920-5861/$ – see front matter © 2008 Elsevier B.V. All rights reserved.
doi:10.1016/j.cattod.2008.08.019

Pt loading. The catalysts were successively dried at 363 K for 5 h (temperature ramp 3 K/min) and calcined in air for 3 h at 773 K (temperature ramp 2 K/min) followed by reduction with $H_2$ (5 vol.% $H_2/N_2$ mixture) for 3 h at 773 K (temperature ramp 2 K/min).

### 2.2. The characterisation of samples

The prepared materials were characterised by X-ray diffraction (XRD) using a TUR M-62 diffractometer ($CuK_\alpha$ radiation, $\lambda = 0.154$ nm). Surface areas, pore diameters and pore volumes of the MCM-41 materials were calculated from low-temperature nitrogen adsorption isotherms measured on a Micromeritics 2010 sorptometer. Prior to adsorption measurements, the samples were degassed in a vacuum at 573 K for 3 h. The same sorptometer was employed, after a slight modification, to measure hydrogen chemisorption. The following procedure was applied in the measurements: preliminary evacuation and heating at 573 K for 1 h, the flow of hydrogen at 573 K for 1 h, evacuation at 573 K for 2 h, cooling down to 308 K, leak test and finally the measurement of hydrogen uptake at 308 K. The linear part of total hydrogen adsorption isotherm was extrapolated to zero pressure to evaluate the saturation of platinum surface with chemisorbed hydrogen. In agreement with Ref. [6], it was assumed that total hydrogen uptake was more suitable than irreversible hydrogen uptake for the calculation of platinum surface area, although some authors prefer to use for this purpose irreversibly bound hydrogen. Platinum surface area ($S$) was calculated from the formula [6]:

$$S = N_0 \alpha \frac{D}{M}$$

where $N_0$ is the Avogadro number, $\alpha$ is area occupied by one atom of platinum, $D$ is dispersion, and $M$ is the atomic weight of platinum. If metal surface area is expressed in $m^2/g$, its density $\rho$ in $g/cm^3$, and spherical shape of metal particles is assumed, then the formula for calculation of mean particle size $P$ is [6]:

$$P = \frac{6000}{S}\rho$$

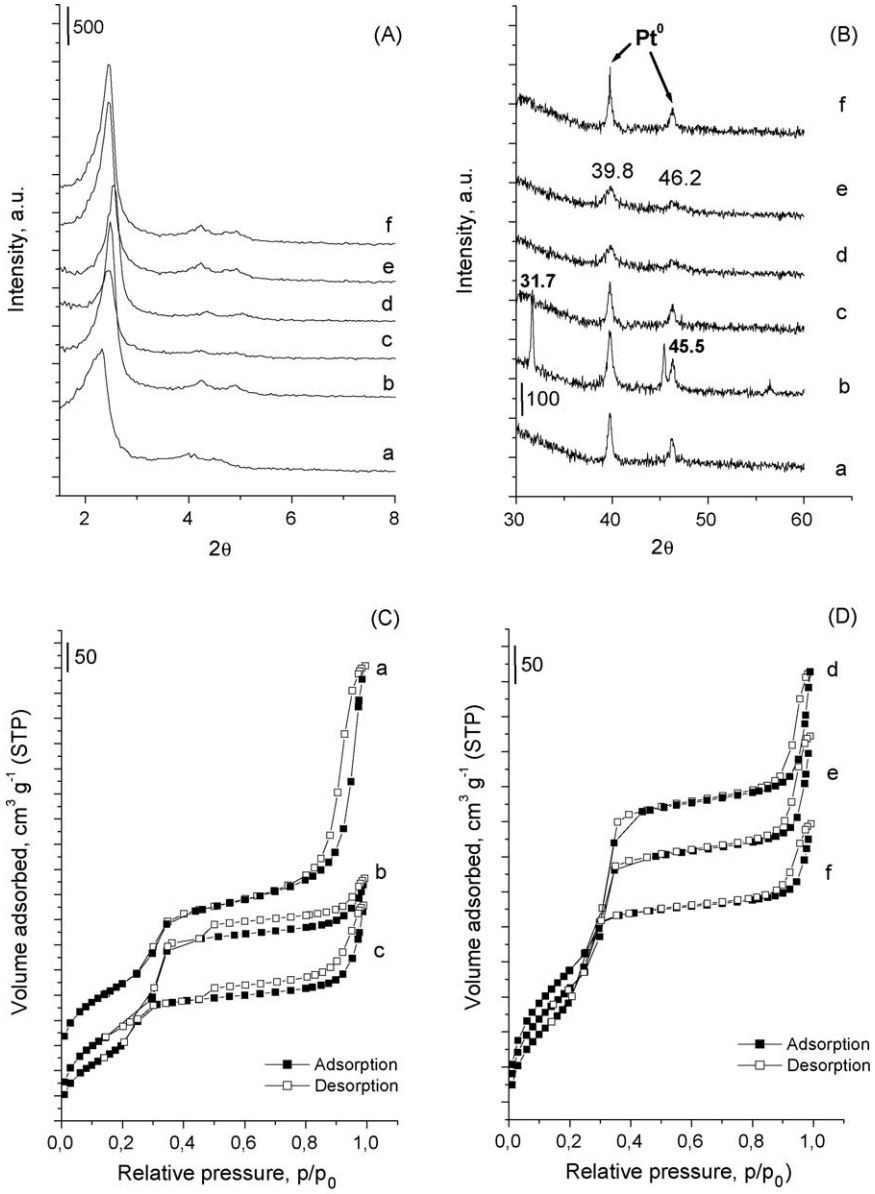


**Fig. 1.** Small-angle (A) and high-angle (B) X-ray diffraction patterns and $N_2$ adsorption/desorption isotherms (C, D) of Pt/Nb(128)MCM-41 (a), Pt/Zr(128)MCM-41 (b), Pt/Zr(256)Nb(256)MCM-41 (c), Pt/Nb(128)/MCM-41 (d), t/Zr(256)/Nb(256)/MCM-41 (e), Pt/Zr(128)/MCM-41 (f).

**Table 1**
Textural parameters of catalysts

| Catalyst[a] | $S_{BET}$ ($m^2/g$) | Mesopore diam. (nm) (from PSD)[b] | Total volume ($cm^3/g$) | Wall thickness ($t$) (nm)[c] |
|---|---|---|---|---|
| Pt/Zr(128)M calc. | 825 | 2.21 | 0.78 | 2.03 |
| Pt/Zr(128)M red. | 787 | 2.06 | 0.72 | 2.26 |
| Pt/Zr(256)Nb(256)M red. | 1020 | 2.89 | 0.91 | 1.82 |
| Pt/Nb(128)M red. | 914 | 2.83 | 1.32 | 1.76 |
| Pt/Nb(128)/M red. | 1005 | 3.33 | 0.71 | 1.83 |
| Pt/Zr(256)/Nb(256)/M red. | 1186 | 3.58 | 0.86 | 1.86 |
| Pt/Zr(128)/M red. | 1043 | 3.07 | 0.69 | 1.82 |

[a] Numbers in brackets indicate Si/metal molar ratio; slash stands for the impregnation method.
[b] PSD—pore size distribution.
[c] $t = a_0 - D/1.05$.

**Table 2**
Platinum dispersion on MCM-41 (denoted as M) supports

| Catalyst[a] | Pt dispersion (%) | Pt surface area ($m^2/g_{metal}$) | Average Pt size from $H_2$ ads. (nm) |
|---|---|---|---|
| Pt/Zr(128)M calc. | 38.3 | 95 | 3.0 |
| Pt/Zr(128)M red. | 31.3 | 77 | 3.6 |
| Pt/Zr(256)Nb(256)M red. | 24.4 | 60 | 4.6 |
| Pt/Nb(128)M red. | 17.4 | 43 | 6.5 |
| Pt/Nb(128)/M red. | 20.9 | 52 | 5.4 |
| Pt/Zr(256)/Nb(256)/M red. | 19.2 | 47 | 5.9 |
| Pt/Zr(128)/M red. | 10.5 | 26 | 10.8 |

[a] Numbers in brackets indicate Si/metal molar ratio; slash stands for the impregnation method.

TEM studies were performed on a JEOL 2000 electron microscope operating at 80 kV, while SEM ones on a Philips SEM 515 operating at 15 kV. Powdered samples were deposited on a grid with a holey carbon film before being transferred to the electron microscope.

## 3. Results and discussion

XRD patterns (Fig. 1A) and TEM images (not shown here) confirmed the hexagonal, well-ordered arrangement of mesopores in all samples used in this study. X-ray diffraction patterns at low-angle range are characteristic of the mesostructured materials with highly ordered hexagonal arrangement [7]. They are characterised by a narrow single Bragg peak (1 0 0) at $2\theta \approx 2^\circ$ and up to three peaks in the region of $2\theta \approx 3$–$8^\circ$.

The presence of Pt-metal clusters can be seen in the high-angle range of XRD patterns (Fig. 1B). The characteristic reflections of metallic platinum at 39.7° ((1 1 1) plane) and 46.2° ((2 0 0) plane) [8,9] are clearly visible in X-ray diffraction patterns of all the materials. In the XRD pattern of Pt/Zr(128)MCM-41 (Fig. 1B-b), additional peaks at 31.7 and 45.5 $2\theta$ degrees are present. They can be indexed to the ZrSi(1 1 1) (JCPDF file 72-1271) and $ZrO_2$(2 1 1) (JCPDF file 86-1451), respectively [10].

The nitrogen adsorption isotherms are typical of mesostructured MCM-41 type materials. The samples prepared via one-pot synthesis in the presence of Zr source (Fig. 1 C-b,c) slightly differ from the others. They exhibit the hysteresis loop characteristic of wide-mouth shaped pores which can be generated as a result of zirconium interaction with silicon that leads to the formation of silicides or oxysilicides.

Textural parameters of all materials used in this study (Table 1) clearly depend on the chemical composition of support, preparation methods as well as zirconium and niobium loading. When zirconium was introduced during the synthesis of MCM-41, thicker walls and small mesopore diameter were obtained, while BET surface area decreased. The wall thickness was calculated assuming the hexagonal pore geometry and the unit cell parameter, $a_0$ ($a_0 = 2\,(3^{-1/2})\,d$), minus the distance, $D$, between the midpoints of the sides of the hexagonal cross-section, equal to $D/1.050$ [11]. Interestingly enough, the materials into which Zr and/or Nb were introduced using wet impregnation of silicate MCM-41 were characterised by large surface areas and pore diameters as well as by relatively thinner walls.

The morphology of MCM-41 materials underwent dramatic changes after the incorporation of zirconium. SEM images show very small and rather uniform particles for all Zr-containing materials into which Zr was introduced during synthesis. The smallest particle sizes of the mesoporous material were observed for the material containing both niobium and zirconium (Fig. 2). The impregnation of NbMCM-41 with zirconium salt has influenced the texture only to a slight extent.

The location of Nb species (extra-framework vs. framework) depends on the method of niobium incorporation into the silicate mesoporous material. The presence of UV band (not shown here) at ~230 nm, originated from tetrahedrally coordinated Nb species [12–14], and the absence of that at ~330 nm, assigned to octahedrally coordinated Nb, in UV–vis spectra of NbMCM-41 prepared by one-pot synthesis indicates that niobium is located in the framework. In contradistinction to that, in the material prepared by the impregnation with Nb salt, niobium oxidic species are anchored to the walls in the extra-framework positions. The zirconium-containing materials exhibit the UV band at ~212 nm, assigned to tetrahedrally coordinated Zr [15–17].

There is no simple relationship between the particle size of mesoporous material (Fig. 2) and platinum dispersion (Table 2) because the chemical compositions of supports have also a significant impact on the latter. The presence of Pt-metal clusters

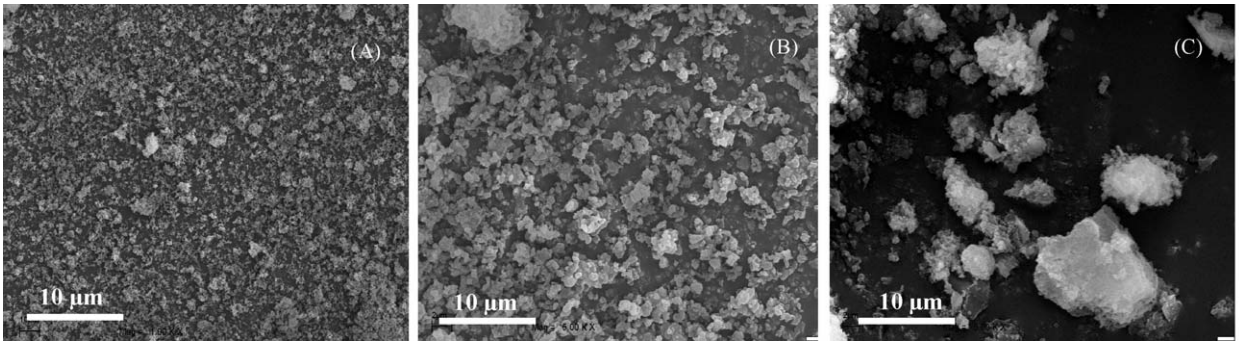


**Fig. 2.** SEM images of Pt/Zr(256)Nb(256)MCM-41 (A), Pt/Zr(128)MCM-41 (B), Pt/Nb(128)MCM-41 (C).

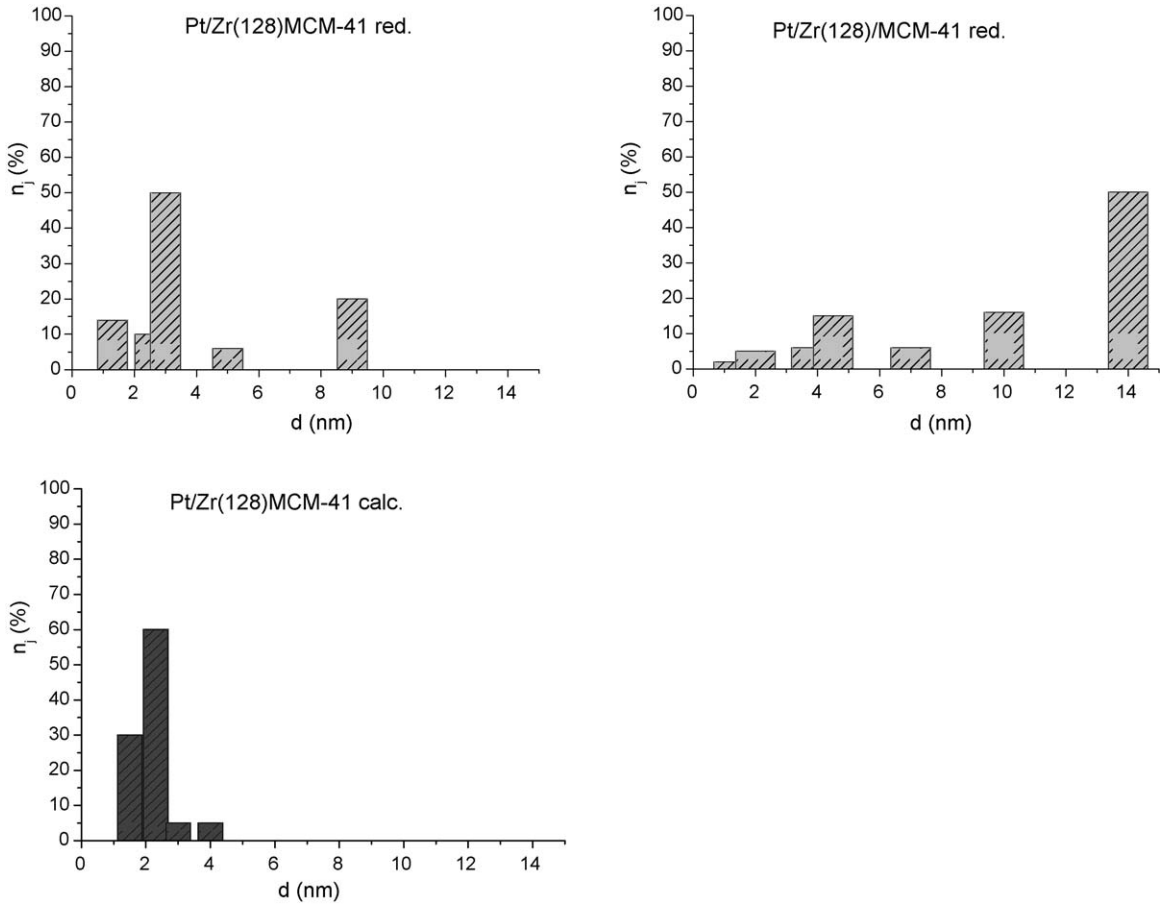


**Fig. 3.** Distribution of platinum particle size on Zr-containing materials.

right after the calcination step is evidenced by high-angle range of XRD patterns [18]. The results shown in Table 2 clearly indicate that the reduction step brings about the agglomeration of Pt clusters and results in a decrease of Pt dispersion. The platinum particle size distribution shown in Fig. 3 confirms the above observation. Interestingly enough, there is a significant difference in the platinum particle size distribution on both reduced Zr-containing samples. In the case of the material modified via impregnation with zirconium salt, that was characterised by bigger particles than those of Zr(128)MCM-41, sintering of platinum proceeds much easier. However, this is not the case of Nb-modified materials. Platinum sintering on niobium-containing supports occurs during the reduction step to a smaller extent than in the case of zirconium-modified samples. This suggests the occurrence of an interaction between platinum species and niobium ones that prevents the agglomeration of metal clusters during the reduction step. However, calcined Pt/Zr(128)MCM-41 shows higher platinum dispersion than its niobium-containing counterpart that is characterised by very large particles size (Fig. 2C) and therefore, even if sintering of Pt during the reduction

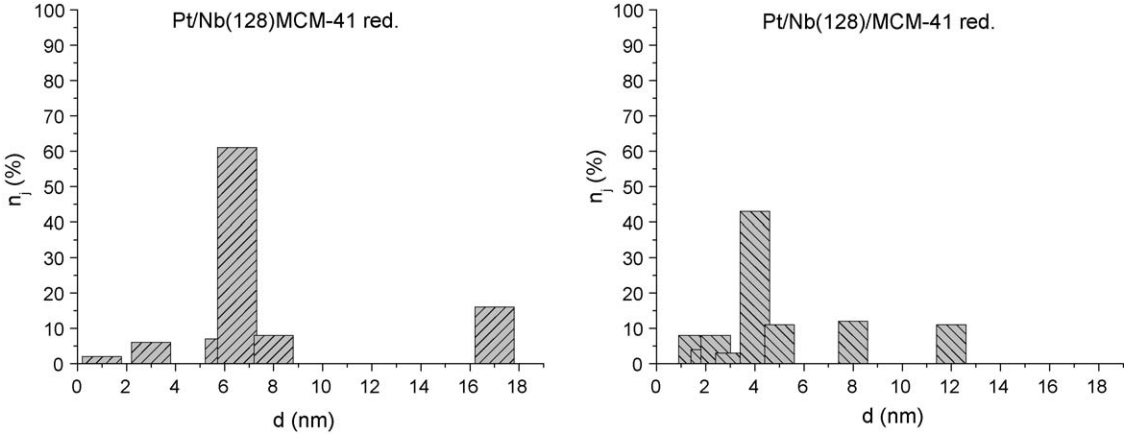


**Fig. 4.** Distribution of platinum particle size on Nb-containing materials.

is faster than that on NbMCM-41 sample, Pt dispersion can be higher in the final reduced sample.

Generally speaking, in the case of the supports onto which Nb and Zr were introduced by one-pot synthesis, the highest Pt dispersion was found on zirconium-containing material. This effect is assigned to particle sizes of the supports. However, when the support was prepared by the impregnation of MCM-41 with the niobium precursor, Pt dispersion after the reduction was much higher than that observed for Pt/Nb(128)MCM-41 (Fig. 4). This indicates that platinum—extra-framework niobium oxide interaction is stronger than that between of platinum and niobium species in the mesoporous walls. This is not the case of Zr species located in the extra-framework positions. This agrees with the well-known fact that strong metal–support interactions (SMSI) were found in the case of $Nb_2O_5$, whereas they were not observed in that of $ZrO_2$ [19].

## 4. Conclusions

Summing up, we wish to emphasize the role of zirconium located in the framework of MCM-41 material (reduction in particle size of the latter) and that of niobium oxide species in the extra-framework positions (the occurrence of SMSI) in the formation of well-dispersed platinum crystallites.

## Acknowledgements

Polish Ministry of Science and Higher Education (grant No. N204 3735 33) and CBMM (Brazil) are acknowledged for the financial support and for supplying Nb source, respectively.

## References

[1] D. Wang, S. Penner, D.S. Su, G. Rupprechter, K. Hayek, R. Schlogl, J. Catal. 219 (2003) 434.
[2] I. Sobczak, M. Ziolek, M. Nowacka, Microporous Mesoporous Mater. 78 (2005) 103.
[3] I. Sobczak, M. Ziolek, J. Goscianska, F. Romero Saria, M. Daturi, J.M. Jablonski, Stud. Surf. Sci. Catal. 158 (2005) 1319.
[4] J. Goscianska, M. Ziolek, Catal. Today 137 (2008) 197.
[5] I. Nowak, M. Ziolek, Chem. Rev. 99 (1999) 3603.
[6] G. Bergeret, P. Gallezot, in: G. Ertl, H. Knozinger, J. Weitkamp (Eds.), Handbook of Heterogeneous Catalysis, vol. 2, VCH, Weinheim, 1997, pp. 440–444, Chap. 3.1.2.
[7] J.S. Beck, J.C. Vartuli, W.J. Roth, M.E. Leonowicz, D.T. Kresge, K.D. Schmitt, C.T.W. Chu, D.H. Olson, E.W. Sheppard, S.B. McCullen, J.B. Higgins, J.L. Schlenker, J. Am. Chem. Soc. 114 (1992) 10834.
[8] S.C. Shen, S. Kawi, Appl. Catal. B 45 (2003) 63.
[9] J. Perez-Ramirez, J.M. Garcia-Cortes, F. Kepteijn, G. Mul, J.A. Moulijn, C. Salinas-Martinez de Lecea, Appl. Catal. B 29 (2001) 285.
[10] J. Goscianska, M. Ziolek, Stud. Surf. Sci. Catal. 165 (2007) 215.
[11] M. Kruk, M. Jaroniec, A. Sayari, J. Phys. Chem. B 101 (1997) 583.
[12] M. Nashimura, K. Asakura, Y. Iwasawa, J. Chem. Soc. Chem. Commun. 15 (1986) 1660.
[13] B. Kilos, A. Tuel, M. Ziolek, J.C. Volta, Catal. Today 118 (2006) 416.
[14] B. Kilos, I. Nowak, M. Ziolek, A. Tuel, J.C. Volta, Stud. Surf. Sci. Catal. 158 (2005) 1461.
[15] K. Chaudhari, R. Bal, T.K. Das, D. Srinivas, A.J. Chandwadkar, S. Sivasanker, J. Phys. Chem. B 104 (2000) 11066.
[16] B.L. Newalkar, J. Olanrewaju, S. Komarneni, J. Phys. Chem. B 105 (2001) 8356.
[17] C. Wang, X. Wang, N. Xing, Q. Yu, Y. Wang, Appl. Catal. A: General 334 (2008) 137.
[18] J. Goscianska, M. Ziolek, Stud. Surf. Sci. Catal. B 170 (2007) 1870.
[19] S.J. Tauster, S.C. Fung, J. Catal. 55 (1978) 29.